Available online at www.sciencedirect.com
SCIENCE DIRECT®
PERGAMON
International Journal of Heat and Mass Transfer 46 (2003) 2603–2614
International Journal of HEAT and MASS TRANSFER
www.elsevier.com/locate/ijhmt

Visualization and measurements of periodic boiling in silicon microchannels

H.Y. Wu, Ping Cheng *

Department of Mechanical Engineering, Hong Kong University of Science and Technology, Clear Water Bay, Kowloon, Hong Kong

Received 27 September 2002; received in revised form 12 December 2002

Abstract

A simultaneous visualization and measurement investigation has been carried out on flow boiling of water in parallel silicon microchannels of trapezoidal cross-section. Two sets of parallel microchannels, having hydraulic diameters of 158.8 and 82.8 μm, respectively, were used. The visualization study shows that once boiling heat transfer is established, two-phase flow and single-phase liquid flow appear alternatively with time in the microchannels. Large-amplitude/long-period fluctuations with time in wall temperatures, fluid temperatures, fluid pressures, and fluid mass flux, are measured for the first time during flow boiling in the microchannels. The fluctuation periods are found to be dependent on channel size, heat flux, and mass flux. The mechanism of the periodic boiling fluctuations in this experiment as well as their comparisons with other boiling fluctuations phenomena reported previously, are also discussed. The experimental results confirm that large-amplitude/long-period boiling fluctuations can be sustained when the fluctuations of pressure drop and mass flux have phase differences.With the aid of a microscope and high-speed video recording system, bubbly flow, slug flow, churn flow, and other peculiar flow patterns, are observed during two-phase flow periods in the microchannels.

Keywords: Boiling heat transfer; Microchannels; Instability

1. Introduction

Recently, there has been a great surge of research activities on boiling heat transfer in microchannels because of the demand for dissipating increasingly higher heat fluxes from electronic, power, and laser devices. Peng and Wang [1] carried out experiments on the flow boiling of water in stainless steel microchannels with the rectangular cross-section of 0.6×0.7 mm. Their experimental results showed that the velocity and liquid subcooling had no obvious effects on the fully developed nucleate boiling,and that no bubbles were observed at a heat flux much greater than 10 W/cm^2 in their experiments.To explain the latter unusual phenomena, Peng and Wang [2] proposed the concepts of "evaporating space" and "fictitious boiling".

Qu and Mudawar [3] measured the incipient boiling heat flux in a copper heat sink containing 21 rectangular microchannels of 231×713 μm using deionized water with inlet velocities of 0.13–1.44 m/s, inlet temperatures of 30, 60, and 90 °C, and an outlet pressure of 1.2 bar. Using a microscope, boiling incipience was identified when bubbles were first detected near the outlet of the microchannels. They found that these bubbles grew and departed into the liquid flow instead of collapsing locally as in larger channels. Both the incipient boiling heat flux and the associated wall superheat increased with increasing inlet velocity and decreasing inlet temperature. The incipient heat flux increased approximately from 10 to 180 W/cm^2 with the wall superheat increasing approximately from 3 to 21 °C as the water velocity was increased from 0.15 to 1.2 m/s at an inlet water temperature of 30 °C. A numerical solution was obtained to

* Corresponding author. Tel.: +852-2358-7181; fax: +852-2358-1543.
E-mail address: mepcheng@ust.hk (P. Cheng).

0017-9310/03/$ - see front matter
doi:10.1016/S0017-9310(03)00039-5

Nomenclature

a	top width of microchannel	V	electric voltage to heater
A_c	cross-sectional area of microchannel	P	pressure
A_w	area of heated wall	t	time
b	bottom width of microchannel	T	temperature
D_h	hydraulic diameter of microchannel	*Greek symbol*	
h	depth of microchannel	φ	heat transfer ratio
L	length of microchannel	*Subscripts*	
m	average mass flux	i	inlet
N	total numbers of microchannels	o	outlet
q	heat flux	w	wall
I	electric current to heater		

predict the incipient boiling heat flux, which was found to be in reasonable agreement with their experimental data.

Jiang et al. [4] carried out visualization and measurements of flow boiling in silicon microchannels of triangular cross-section, having hydraulic diameters of 26 and 53 μm respectively. In their experiments, the heater was located upstream of the microchannels. They observed that local nucleation boiling occurred in the microchannels at a low input power of $Q/Q_{CHF} = 0.4$. They found the stable annular flow occurred at a higher input power in the range of $0.6 < Q/Q_{CHF} < 0.9$, and no bubbly flow was observed in their microchannels. Zhang et al. [5] carried out an experiment on flow boiling in silicon rectangular microchannels having $D_h = 25$–60 μm. They found that boiling occurred with less than 5 °C of superheat and they observed mostly annular flow with a very thin layer of liquid. However, the bubbly and slug flows typically observed in the macrochannels were absent from their experiment. Hetsroni et al. [6] investigated flow boiling of water in the silicon triangular microchannels having hydraulic diameters of 103 and 129 μm respectively. Their experiments were carried out at a heat flux in the range of 8–36 W/cm^2 and at a Reynolds number from 20 to 75. They mentioned that two types of periodic flow patterns were observed: the periodic annular flow and the periodic dry steam flow. However, no fluctuation data of pressure or temperature were reported in their paper. In a more recent paper, Hetsroni et al. [7] reported short-period (in the order of 1–2 s) and low-amplitude oscillation data in pressure drop and outlet temperature at $q = 3.2$ W/cm^2 and $m = 14.8$ g/cm^2 s, as well as at $q = 3.6$ W/cm^2 and $m = 14.8$ g/cm^2 s, respectively. Their experiments were performed on flow boiling of the Vertrel XF fluid in silicon microchannels of triangular cross-section, having a hydraulic diameter of 130.14 μm. The low-amplitude/short-period fluctuations in the pressure drop and outlet fluid temperature were attributed to the growth and collapse of vapor fraction. Most recently, some reports on boiling instability in the small channels with dimensions ranging from 889 μm to 5 mm began to appear [8–10]. However, no paper has reported large-amplitude/long period boiling fluctuations in microchannels having a hydraulic diameter less than 500 μm.

In this paper, flow boiling of water in the parallel silicon microchannels having trapezoidal cross-sectional area, with hydraulic diameters of 158.8 μm (microchannels #1) and 82.8 μm (microchannels #2) respectively, is studied by simultaneous measurements and flow visualization techniques. It was observed that once boiling heat transfer is established, single-phase and two-phase flow alternates in the microchannels. Large-amplitude/long-period fluctuations in wall temperatures, fluid temperatures, fluid pressures, and fluid mass flux in microchannels #1 (at $q = 13.0$ W/cm^2 and $m = 14.4$ g/cm^2 s) and microchannels #2 (at $q = 7.83$ W/cm^2 and $m = 16.8$ g/cm^2 s) were measured. These large-amplitude/long-period fluctuations are compared with pressure and temperature fluctuations in macrochannels reported previously [11–15]. With the aid of a microscope and high-speed video recording system, it was observed that the bubbly flow, slug flow, churn flow or other peculiar flow patterns may occur in the microchannels during two-phase flow periods.

2. Description of the experiment

2.1. Experimental system

Fig. 1 shows the experimental setup used in the present investigation. A pressure tank was used to ensure flow stability before entering the test section and to ensure enough pressure in driving the liquid in the microchannels. The deionized and degassed water in the pressure tank, being pushed by the compressed nitrogen

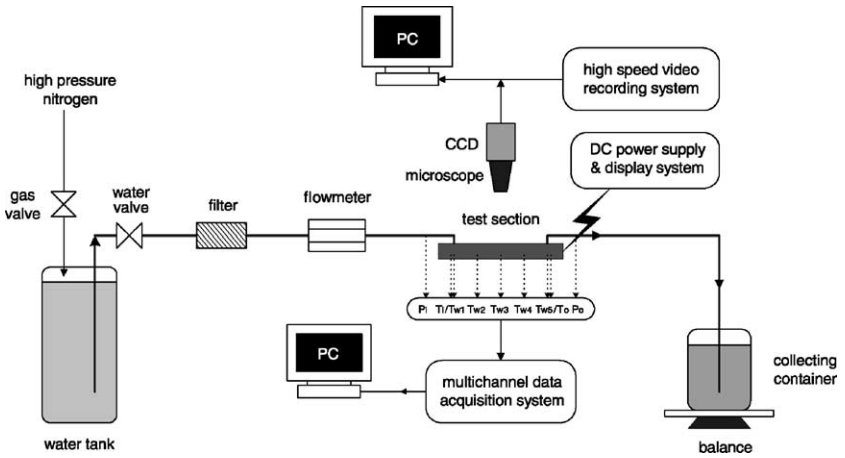

Fig. 1. Experimental setup.

gas, flowed successively through a valve regulator, a filter, a flowmeter, to the test section, and finally was collected and condensed in a container with a small hole vented to the atmosphere. The container was placed on a precision balance, and the average mass flux of water was determined by calculating the mass increment per unit time. Using this primary weighing method, the flowmeter used for the determination of instantaneous mass flux in this experiment was calibrated.

2.2. Test section

The test section is shown schematically in Fig. 2. The $\langle 100 \rangle$ silicon wafer with parallel microchannels was first anodically bonded from the top with a thin pyrex glass plate. It was then placed in a teflon base, which had already been attached by a thermal-insulating layer, a film heater, and an electric-insulating film at its bottom. The thickness of the pyrex glass, silicon wafer, electric-insulating film, film heater, and thermal-insulating layer were 0.5, 0.525, 0.1, 0.1, and 3 mm, respectively. To ensure constant heating with respect to time, the film heater was energized by a DC power supply, which could be regulated in the ranges of 0–30 V and 0–3 A. At the bottom of the silicon wafer, five type-T thermocouples of 0.1 mm in diameter, being evenly spaced from the channels' inlet to outlet, were attached. The electric-insulating film, sandwiched between the silicon bottom and the film heater, was a thermal-conductor. Therefore, it could assure good heat transfer from the film heater to the silicon wafer while insulating effectively the thermocouple signal from the film heater. Finally, a transparent polycarbonate plate with inlet and outlet holes for water was aligned and secured to the teflon base, leaving a leak-proof contact with the pyrex glass through two O-rings. The locations for the measurements of inlet and outlet water temperatures as well as wall temperatures are shown in Fig. 2.

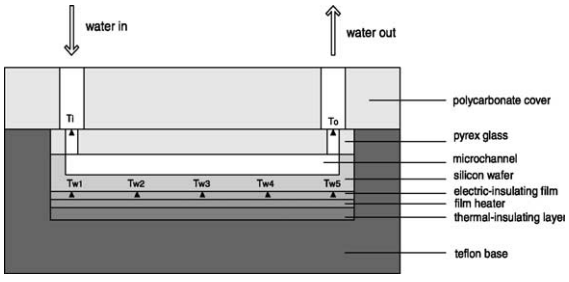

Fig. 2. Test section.

2.3. Measurement system

Water temperatures at the inlet and outlet of the microchannels were measured by two type-T thermocouples having a diameter of 0.25 mm and a response time of 0.2 s. The wall temperatures of the microchannels were measured by five type-T thermocouples, having a diameter of 0.1 mm and a response time of 0.1 s. Water pressures at the inlet and outlet of the microchannels were measured by two pressure transducers having an accuracy of $\pm 0.04\%$ and a response time of 0.001 s. The average mass flux of water was obtained by the primary weighing method discussed earlier. The instantaneous mass flux was measured by a flowmeter located upstream of the test section. The flowmeter, having a range of 200 ccm, a response time of 0.02 s, and an accuracy of $\pm 2\%$ full scale, was calibrated by the primary weighing method as mentioned above. Instantaneous measurements in temperatures, pressures, and water mass flux were collected by a data acquisition

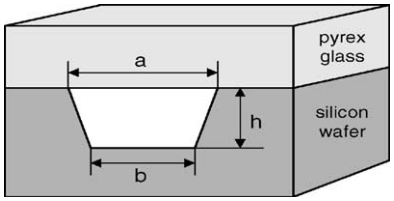

Fig. 3. Cross-section of a trapezoidal microchannel.

system, and displayed by a PC monitor or stored in PC memory for further analyses.

2.4. Visualization system

Above the test section, a microscope, a CCD adaptor, and a high-speed video recording system were installed (see Fig. 1). The boiling images captured by the high-speed video system were stored and displayed by a PC through an image-capturing card and image-processing software. The image recording and the data collection were carried out at the same time during the experiment, making it possible to compare visual images with measurements.

2.5. Geometric parameters of microchannels

The trapezoidal microchannels in the $\langle 100 \rangle$ silicon wafer were fabricated by the photolithography method. Because of the method's low cost and high precision, microchannels of trapezoidal cross-sections have been widely used in various silicon-base microsystems such as biochip, micropower generator, microfuel cell, etc. Fig. 3 shows the trapezoidal cross-section of the microchannel, where "a" denotes the top width, "b" the bottom width, and "h" the depth of the microchannel. The silicon microchannels were bonded with a pyrex glass plate from the top. Triangular and rectangular cross-sections are two special kinds of the trapezoidal cross-section with $b = 0$ and $b = a$, respectively. Using a surface profiler, the top width a, bottom width b, as well as the depth h of the trapezoidal microchannels were measured. The surface roughness was determined by an atomic force microscope (AFM). Table 1 lists the geometric parameters and the surface roughness of the two kinds of microchannels used in this experiment. As shown in the table, the hydraulic diameter of microchannels #1 with $D_h = 158.8$ μm is larger than that of microchannels #2 with $D_h = 82.8$ μm. Since the wall roughness of these two microchannels is so small (51.8 and 25.2 Å), respectively, they can be regarded as smooth channels.

Table 1
Geometric parameters of microchannels

Channel	#1	#2
a (μm)	431.2	159.7
b (μm)	267.5	35.9
h (μm)	110.7	86.3
D_h (μm)	158.8	82.8
Roughness (Å)	51.8	25.2
N	8	15

2.6. Experimental procedure

Before the experiment, the following preparations are made:

1. Install the test wafer into the test section.
2. Close all valves in the system.
3. Fill the pressure tank with the deionized and degassed water.
4. Fill cooling water into the collecting container.
5. Adjust the zero reading of the flowmeter at atmospheric pressure corresponding to a "no flow" condition.

After above preparations have been completed, the experiment is carried out as follows:

1. Open the gas valve and maintain the pressure tank at a fixed pressure.
2. Open the water valve carefully and slowly until the water pressure at the inlet of microchannels reaches the predetermined value.
3. Leave the water flowing through the system for some time until the gas bubbles inside the system have been completely removed from the system.
4. Open the DC power supply source and keep its voltage and current outputs at predetermined values.
5. Leave the system unchanged for about thirty minutes, then record the initial weight of collecting container on the balance, and at the same time starts timing.
6. Make a simultaneous record of temperature, pressure and mass flow measurements, while the video system is recording boiling images in the microchannels.
7. After the timer has been turned on for about thirty minutes, record the weight of collecting container on the balance, and at the same time turn off the timer.
8. Leave other parts of the system unchanged, and increase the DC power supply output to a new level.
9. Repeat the process from 5 to 8.
10. Terminate the experiment.

2.7. Accuracy of heat flux and average mass flux measurements

The heat flux, q, is computed by $q = \varphi VI/A_w$, where V and I are the input voltage and current to the film heater, A_w is the area of heated wall, and φ is the ratio of

the heat absorbed by the water to the total power input to the film heater. The value of φ was determined by a method similar to that used by Hetsroni et al. [6,7]. The average mass flux of water is given by $m = \Delta M/(\Delta t \cdot N \cdot A_c)$, where ΔM is the total mass increment in the container measured by the balance during the time interval Δt, N is the total number of microchannels, and A_c is the cross-sectional area of a microchannel.

The uncertainties in determining q and m can be determined from the measurement uncertainties of V (0.45%), I (0.59%), φ (2.71%), A_w (2.01%), ΔM (2.40%), Δt (0.11%), and A_c (2.18%). Performing the standard error analysis, the uncertainties of q and m were 5.76% and 4.69%, respectively.

3. Discussion of experimental results

3.1. Experimental results for microchannels #1

Figs. 4–8 present the experimental results for microchannels #1 having a hydraulic diameter of 158.8 μm.

3.1.1. Temperature fluctuations

When the heat flux was raised gradually while keeping other conditions (tank pressure, tank temperature, container pressure, valve open level, and etc.) unchanged, different flow patterns were observed, and at the same time, different temporal variations of temperatures were recorded. When the heat flux was maintained at 5.78 W/cm^2 with a corresponding mass flux of

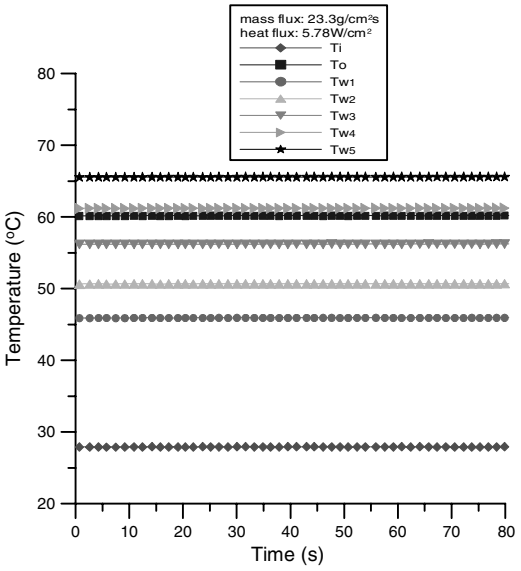

Fig. 4. Wall and fluid temperatures in microchannels #1 during single-phase liquid flow.

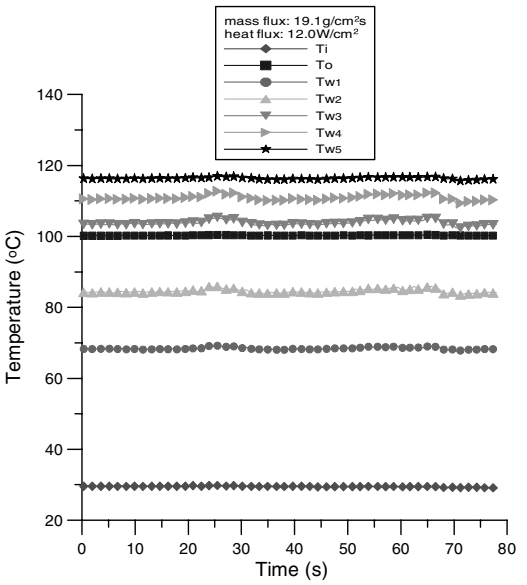

Fig. 5. Wall and fluid temperatures in microchannels #1 at incipient boiling.

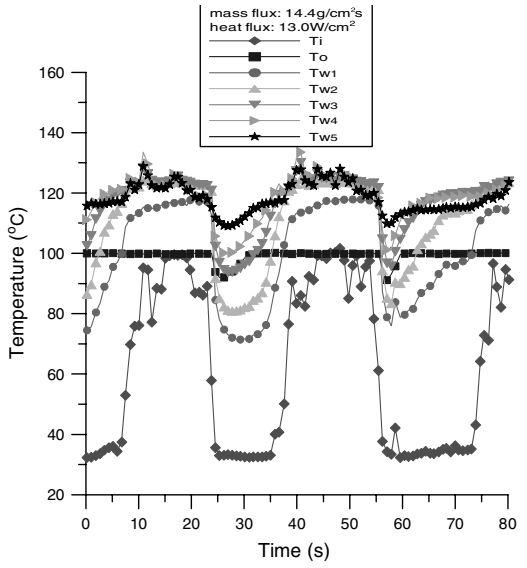

Fig. 6. Temperature fluctuations in microchannels #1 during periodic boiling.

23.3 g/cm^2 s, the fluid in the microchannels was in the liquid phase. Under this situation, all temperature measurements (including inlet/outlet fluid temperatures and the five wall temperatures) remained constant with time, which are presented as straight lines in Fig. 4. However, as the heat flux was increased to 12.0 W/cm^2 with a corresponding mass flux of 19.1 g/cm^2 s as shown

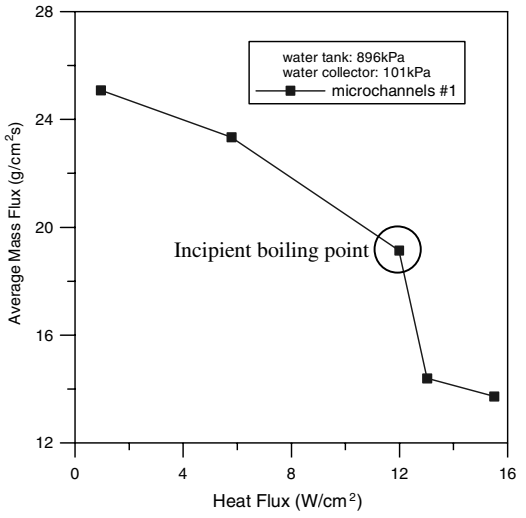

Fig. 7. Average mass flux vs heat flux in microchannels #1 around incipient boiling point.

in Fig. 5, some vapor bubbles began to appear near the channel outlet, and a small temporal fluctuation of wall temperatures was observed. This is referred to as the incipient boiling. The incipient boiling heat flux of 12.0 W/cm^2 determined from this experiment is of the same order of magnitude obtained by Qu and Mudawar [3] under similar experimental conditions. It is shown from Fig. 5 that at the incipient boiling state, the outlet fluid temperature T_o reached the saturation value of 100 °C corresponding to the outlet atmospheric pressure, while the inlet fluid temperature T_i was at 30 °C, which was hardly affected by boiling at the outlet.

When the heat flux was further increased to 13.0 W/cm^2 with an average mass flux of 14.4 g/cm^2 s, boiling occurred almost everywhere in the microchannels. At the same time, large temporal fluctuations of temperatures were recorded as shown in Fig. 6. It is found that: (1) among all temperature fluctuations, the inlet water temperature fluctuated most acutely (with an amplitude about 70 °C), the outlet water temperature fluctuated moderately (with an amplitude about 10 °C), and the fluctuation amplitude of various wall temperatures lied in between (from 20 to 50 °C); (2) temperature fluctuations at various locations were almost in phase, at a fluctuation period of approximately 31 s; (3) in addition to large-amplitude fluctuations with a long period (in the order of 30 s), there existed small-amplitude fluctuations with a short period (in the order of seconds) in inlet water temperature and in some wall temperatures during two-phase flow periods. These small-amplitude/short-period fluctuations were mainly caused by the bubble dynamic instabilities during the two-phase flow period.

3.1.2. Average mass flux vs heat flux relations

Fig. 7 shows that the *average* mass flux of water decreased from 25.1 to 13.7 g/cm^2 s when the heat flux was increased from 0.96 to 15.5 W/cm^2, while keeping other conditions in the system unchanged. The decrease of mass flux from 25.1 to 23.3 g/cm^2 s during single-phase liquid flow is mainly because of the decrease in water density due to temperature increase. The decrease of mass flux from 23.3 to 19.1 g/cm^2 s was caused initially by the decrease in fluid density, and later by the generation of a small amount of bubbles near the channel outlet. An abrupt decrease in the mass flux from 19.1 to 14.4 g/cm^2 s was mainly due to the generation of a large amount of bubbles in the whole test section.

3.1.3. Visualization of periodic boiling

During the temperature data collection process, the periodic boiling phenomena in the microchannels #1 were recorded simultaneously by a high-speed video recording system, which was located above the mid length of the microchannels. Fig. 8 shows some typical video pictures corresponding to Fig. 6 at a heat flux of 13.0 W/cm^2 and an average mass flux of 14.4 g/cm^2 s. The time shown in Fig. 8 and the time shown in Fig. 6 are one-to-one correspondence. It can be seen that: (1) the single-phase liquid flow and two-phase flow appeared alternatively in the microchannels once boiling is established. Fig. 8a shows that the single-phase liquid flow existed during $t = 0$ to 7 s. From $t = 7$ to 24 s, the microchannels were occupied by the two-phase flow: Fig. 8b shows the bubbly flow occurring at $t = 15$ s while Fig. 8c shows a new type of two-phase flow occurring in the microchannels at $t = 20$ s. As shown in Fig. 8d, single-phase liquid flow appeared again from $t = 24$ to 38 s in the microchannels. This was followed by another two-phase flow period which lasted about 18 s from $t = 38$ to 56 s: Fig. 8e shows a peculiar two-phase flow pattern occurring at $t = 45$ s and Fig. 8f shows the bubbly flow at $t = 50$ s. At the end of this two-phase flow period, the single-phase liquid flow in Fig. 8g appeared again, which lasted about 18 s. Beginning from $t = 74$ s, the two-phase flow occurred again, and Fig. 8h shows the new two-phase flow pattern occurring at $t = 78$ s again. The above alternation from single-phase liquid flow to two-phase flow repeated itself as time continued; (2) corresponding to the alternation from single-phase liquid flow to two-phase flow, the fluid and wall temperatures show large-amplitude/long-period fluctuations from the trough to the crest; (3) the fluctuation period of various temperatures was consistent with the alternation period of single-phase liquid flow to two-phase flow, which was about 31 s at $q = 13.0$ W/cm^2 and $m = 14.4$ g/cm^2 s in microchannels #1; (4) during two-phase flow periods, the bubbly flow, and some peculiar flow patterns shown in Figs. 8c, e and h, were observed in microchannels #1. These new two-phase flow patterns are absent in macrochannels and

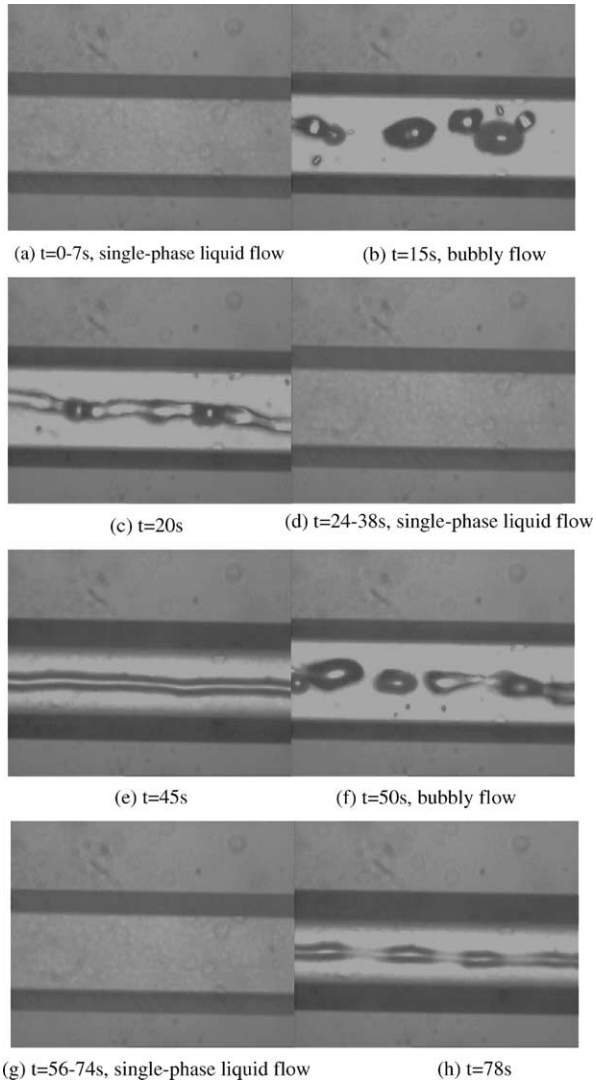

Fig. 8. Photos of periodic boiling in microchannels #1 at $q = 13.0$ W/cm^2 and $m = 14.4$ g/cm^2 s.

need further investigation; (5) during the two-phase flow period, the generation, growth, coalescence and departure of vapor bubbles (usually occurring in macrochannels) were also observed in microchannels #1; and it was this bubble dynamic instabilities that caused small-amplitude and short-period fluctuations in inlet water temperature and some wall temperatures during two-phase flow periods.

3.1.4. Explanation of periodic boiling in microchannels

The reason for alternative appearance of the single-phase liquid flow and two-phase flow in the microchannels can be explained as follows: when boiling occurs in the test section, the pressure drop across the test section suddenly increases due to generation of vapor bubbles. This increase in pressure drop causes the decrease in mass flux, which in turn causes the decrease in pressure drop. Therefore, pressure and mass flux fluctuations occur. During the period of increasing mass flux, the constant heat flux is insufficient to boil the incoming mass flow of water, and consequently the single-phase liquid flow appears. When the mass flux is decreased, the constant heat flux is sufficient to boil the incoming flow of water, which results in a two-phase flow. Thus, single-phase liquid flow and two-phase flow appear alternatively in the microchannels, causing large-amplitude/long-period fluctuations in fluid temperatures and wall temperatures as shown in Fig. 6. According to

the analysis by Wang et al. [12], when the fluctuation of pressure drop and the induced fluctuation of mass flux have phase differences, the fluctuations of pressure drop, mass flux, and wall temperature can be sustained.

3.2. Experimental results for microchannels #2

Experimental results for boiling fluctuations in microchannels #2, having a smaller hydraulic diameter of 82.8 μm, are presented in Figs. 9–12. In addition to temperature fluctuation measurements, temporal fluctuations of the inlet/outlet pressures and instantaneous mass flux were also measured.

3.2.1. Temperature fluctuations

Fig. 9 shows similar temporal fluctuations of fluid temperatures and wall temperatures in microchannels #2 at a heat flux of 7.83 W/cm^2 and an average mass flux of 16.8 g/cm^2 s. It is seen that: (1) corresponding to the large fluctuations of inlet fluid temperature (with an amplitude about 65 °C) and zero fluctuation of outlet fluid temperature, wall temperature fluctuations decayed along the flow direction, from an amplitude of about 45 °C at the location near the inlet to an amplitude of about 10 °C at the location near the outlet; (2) the fluctuation period of water in microchannels #2 was about 141 s, much longer than those in microchannels #1, which was about 31 s as shown in Fig. 6. Since the inlet water subcooling of these two microchannels was the same (about 70 °C), the difference in fluctuation periods can be attributed to the differences in channel size ($D_h = 82.8$ μm vs 158.8 μm), heat flux (7.83 W/cm^2 vs 13.0 W/cm^2), and mass flux (16.8 g/cm^2 s vs 14.4 g/cm^2 s) in the experiments; (3) The inlet thermocouple (see Fig. 1) could measure the instantaneous jump in the fluid temperature that was caused by the alternation of single-phase liquid flow to two-phase flow in microchannels. During the two-phase period, the inlet fluid temperature fluctuated with small amplitudes at short periods. During the single-phase period, the fluid temperature was maintained approximately at the value of 30 °C. Thus, the fluid temperature variation was of U-shape during a cycle.

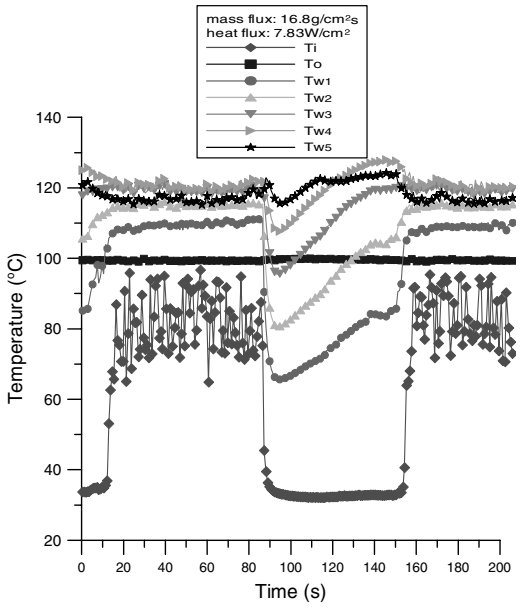

Fig. 9. Temperature fluctuations in microchannels #2 during periodic boiling.

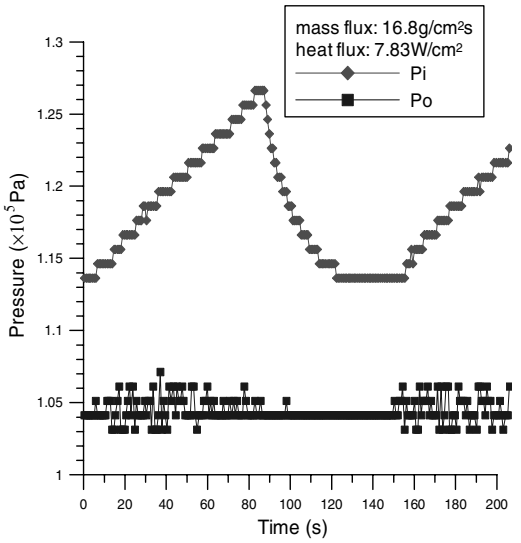

Fig. 10. Pressure fluctuations in microchannels #2 during periodic boiling.

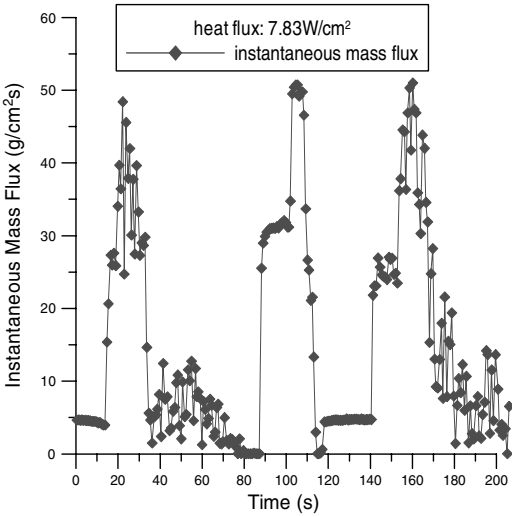

Fig. 11. Mass flux fluctuations in microchannels #2 during periodic boiling.

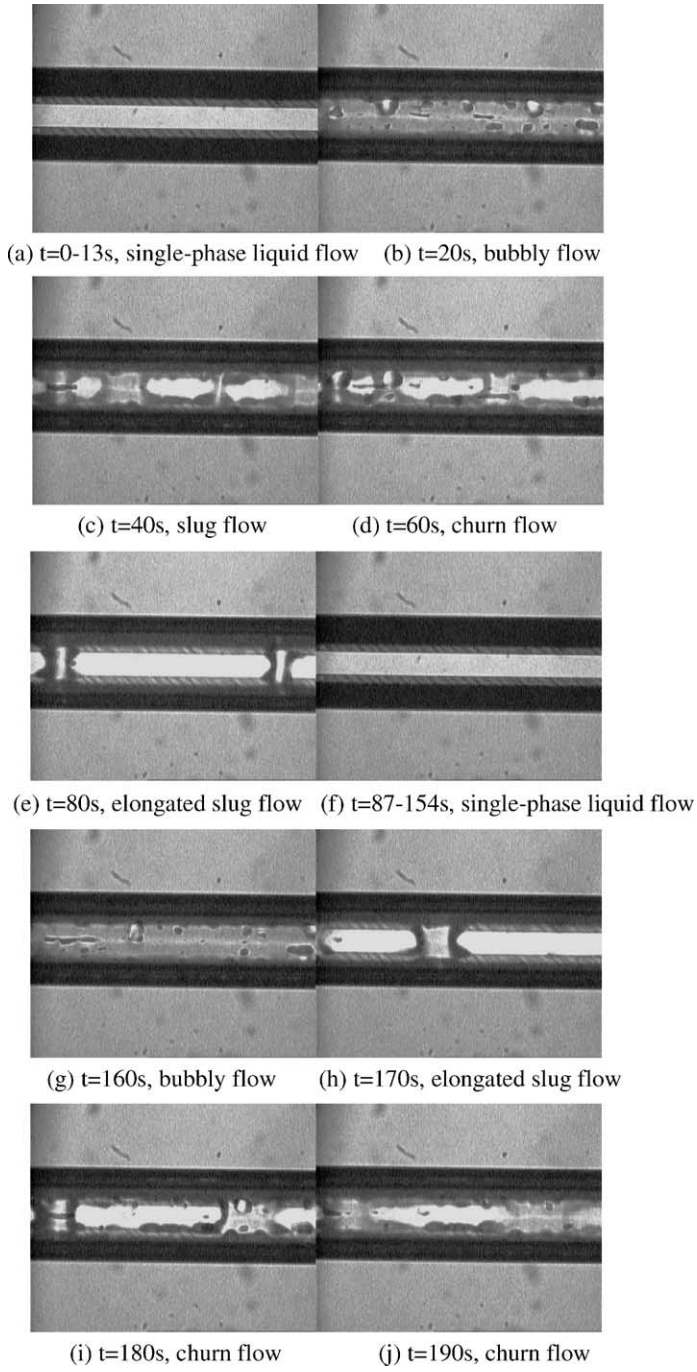

Fig. 12. Photos of periodic boiling in microchannels #2 at $q = 7.83$ W/cm^2 and $m = 16.8$ g/cm^2 s.

3.2.2. Pressure fluctuations

Fig. 10 shows the pressure fluctuations at the inlet and outlet of microchannels #2 at a heat flux of 7.83 W/cm^2 and an average mass flux of 16.8 g/cm^2 s. It is seen that (1) corresponding to the large-amplitude fluctuation of inlet temperature, the inlet pressure fluctuated with an amplitude about 13.2 kPa. Since the outlet of the microchannels was vented to the atmosphere, the outlet pressure had a small fluctuation amplitude about 4 kPa; (2) the period and phase of the pressure fluctuations were the same as those of the temperature fluctuations; (3) since the inlet pressure transducer was located at the

upstream of microchannels' inlet (see Fig. 1), short-period (or high-frequency) pressure fluctuations were not observed. The pressure variation is in V-shape because of its gradual increasing and decreasing values.This V-shape variation in pressure differs from the U-shape variation in fluid temperature as mentioned earlier.

3.2.3. Mass flux fluctuations

Fig. 11 gives the temporal fluctuation of instantaneous mass flux measured by the flowmeter located ahead of the test section of the microchannels #2 at the heat flux of 7.83 W/cm^2 and the average mass flux of 16.8 g/cm^2 s. It is seen that (1) the mass flux also fluctuated with respect to time, with a maximum amplitude of about 50.0 g/cm^2 s; (2) the period of mass flux fluctuations was about 141 s, which was the same as that of temperature and pressure fluctuations; (3) the fluctuations of pressure and mass flux were nearly out of phase, which confirms with the analysis by Wang et al. [12] that the long-period boiling fluctuations could be sustained when the fluctuations of pressure drop and fluctuations of mass flux have phase differences.

3.2.4. Visualization of periodic boiling

As in microchannels #1, the periodic boiling in microchannels #2 was also observed. Fig. 12 shows some typical video pictures on flow boiling of water in microchannels #2 at a heat flux of 7.83 W/cm^2 and an average mass flux of 16.8 g/cm^2 s. The time in Fig. 12 and the time in Figs. 9–11 are one-to-one correspondence. It is seen that (1) the single-phase liquid flow and two-phase flow also appeared alternatively with time at a given location in microchannels #2. Fig. 12a shows the single-phase liquid flow during the time interval of 0–13 s. From $t = 13$ to 87 s, microchannels #2 were occupied by the two-phase flow whose flow patterns were somewhat different from those in microchannels #1: Fig. 12b shows the bubbly flow at $t = 20$ s; Fig. 12c shows the slug flow at $t = 40$ s; Fig. 12d shows the churn flow at $t = 60$ s; and Fig. 12e shows the elongated slug flow at $t = 80$ s. Fig. 12f shows that the single-phase liquid flow appeared again from $t = 87$ to 154 s, which was successively followed by another two-phase flow period again. Figs. 12g–j show some typical flow patterns of this two-phase flow period: Fig. 12g shows the bubbly flow at $t = 160$ s; Fig. 12h shows the elongated slug flow at $t = 170$ s, while Figs. 12i and j show the churn flow at $t = 180$ and 190 s, respectively. As time goes on, the above alternation from single-phase liquid flow to two-phase flow repeats itself; (2) the alternation period of single-phase liquid flow to two-phase flow in microchannels #2 at $q = 7.83$ W/cm^2 and $m = 16.8$ g/cm^2 s was about 141 s, which was the same as the fluctuation period of temperature, pressure and mass flux measurements shown in Figs. 9–11. This consistency in fluctuation periods proved once again that the large-amplitude and long-period fluctuations in temperature, pressure and mass flux measurements were caused by the alternation of single-phase liquid flow to two-phase flow, and not caused by the bubble dynamic instabilities; (3) a comparison of Figs. 9–12 shows that the single-phase liquid flow usually appeared in the period when inlet pressure is falling while the instantaneous mass flux is rising whereas the two-phase flow usually appeared in the period when inlet pressure is increasing while the instantaneous mass flux is decreasing; (4) in microchannels #2 with the hydraulic diameter as small as 82.8 μm, the generation, growth, coalescence and departure of bubbles were also observed during the two-phase flow period, which led to low-amplitude/short-period fluctuations in the inlet temperature (as shown in Fig. 9) and in the instantaneous mass flux (as shown in Fig. 11); (5) during the two-phase flow period, bubbly flow, slug flow, and churn flow were observed in microchannels #2. A comparison of two-phase flow patterns in microchannels #1 and microchannels #2 shows that the slug flow and churn flow occurred more easily in smaller microchannels #2 at $q = 7.83$ W/cm^2 and $m = 16.8$ g/cm^2 s,and the new flow patterns shown in Figs. 8c, e and h,were not observed in microchannels #2 under the experimental conditions.This suggests that the side-walls may have strong effects on the two-phase flow pattern in a smaller microchannel.

4. Comparison of various boiling oscillations

Fluctuations or oscillations in flow boiling in *macrochannels* have been investigated extensively in the past, and three types of oscillations in macrochannels have been discussed [11]: pressure-drop type oscillations, density-wave type oscillations, and thermal oscillations. Pressure-drop type oscillations occur in the boiling two-phase flow systems where the amount of upstream compressible volume is significant, and the amplitude and period of this type oscillations are usually large, and the oscillations of pressure and mass flux are out of phase. Density-wave type oscillations are the most common type of dynamic instabilities related to kinematic wave-propagation phenomena. The amplitude and period of the density-wave type oscillations are generally small, and their pressure and mass flux oscillations are in phase. Thermal oscillations are compound dynamic instabilities related to the instability of the liquid film next to the walls having temperature fluctuations. Though the amplitude of wall temperature oscillations is large, the amplitudes and periods of pressure and mass flux oscillations in thermal oscillation are very small. Besides the above three types of oscillations, Wang et al. [12] observed a new type of dynamic instability in a forced-convection upflow boiling system, which is referred to as "boiling onset oscillations". This new type of oscillation

was found to occur at the onset of the boiling point of the working fluid, and has much longer period and larger amplitude than the density-wave and pressure-drop type oscillations.

Recently, some researchers [7–10] reported small-period (in the order of 0.5–2 s) fluctuations in flow boiling in micro or mini-channels. However, the long-period/large-amplitude fluctuations in temperature, pressure, mass flux due to the alternation of single-phase liquid flow to two-phase flow, as observed in this experiment, are much different from these short-period fluctuations. Also, because no compressible volume existed in the upstream of test section, the long-period/large-amplitude fluctuations in this experiment are not pressure-drop type oscillations.

From the fluctuation amplitude and period shown in Figs. 6,9–11, it appears from the first glance that the boiling fluctuations observed in this experiment are similar to "boiling onset oscillations" observed by Wang et al. [12] and the "periodic circulation oscillations" observed by Kim and Lee [15]. However, a further comparison of fluctuation shape shows that the oscillations occurring in the present experiment are somewhat different from those observed by Wang et al. [12] and by Kim and Lee [15]. Up to now, no similar long-period/large-amplitude fluctuations have been reported in the literature for boiling in microchannels.

5. Concluding remarks

In this paper, a simultaneous visualization and measurement study has been performed on flow boiling of water in two sets of parallel trapezoidal microchannels, having hydraulic diameters of 158.8 and 82.8 μm respectively. The following conclusions are obtained:

1. Two-phase flow and single-phase liquid flow appear alternatively in microchannels, which leads to large-amplitude/long-period fluctuations with time in temperatures, pressures and mass flux. The single-phase flow period corresponds to the period of decreasing pressure drop and increasing instantaneous mass flux whereas the two-phase flow period corresponds to the period of increasing pressure drop and decreasing instantaneous mass flux. These large-amplitude/long-period periodic boiling fluctuations in microsystems are reported in this paper for the first time.
2. The fluctuations of various temperatures and pressures were in phase, but the fluctuations of pressure and mass flux were out of phase. The latter sustained the periodic boiling fluctuation phenomena in microchannels.
3. During the period when inlet pressure was rising while the instantaneous mass flux was falling, there existed small-amplitude/short-period fluctuations in inlet temperature and in instantaneous mass flux due to the bubble dynamic instabilities in the two-phase flow.
4. The boiling fluctuation periods in microchannels #1 and #2 were 31 and 141 s, respectively. The difference in fluctuation periods in these microchannels can be attributed to the differences in channel size, heat flux, and mass flux in the experiments.
5. It was found that slug flow and churn flow occurred more frequently in smaller microchannels #2 under the experimental conditions of $q = 7.83$ W/cm^2 and $m = 16.8$ g/cm^2 s. Some new peculiar flow patterns have been found in larger microchannels #1 under the experimental condition of $q = 13.0$ W/cm^2 and $m = 14.4$ g/cm^2 s. The occurrence of these peculiar two-phase flow patterns needs further investigation. The bubbly flow, which was not observed in previous papers [1,2,4–7], was easily observable in both microchannels #1 and microchannels #2 under the experimental conditions.

Acknowledgements

The authors gratefully acknowledge the support of this work through grants No. HIA98/99.EG04 and HKUST6014/02.

References

[1] X.F. Peng, B.X. Wang, Forced-convection and flow boiling heat transfer for liquid flowing through microchannels, Int. J. Heat Mass Transfer 36 (14) (1993) 3421–3427.
[2] X.F. Peng, B.X. Wang, Evaporation space and fictitious boiling for internal evaporation of liquid, Science Foundation in China 2 (1994) 55–59.
[3] W. Qu, I. Mudawar, Prediction and measurements of incipient boiling heat flux in microchannel heat sinks, Int. J. Heat Mass Transfer 45 (2002) 3933–3945.
[4] L. Jiang, M. Wong, Y. Zohar, Forced convection boiling in a microchannels heat sink, J. Microelectromech. Syst. 10 (1) (2001) 80–87.
[5] L. Zhang, J.M. Koo, L. Jiang, M. Asheghi, K.E. Goodson, J.G. Santiago, Measurements and modeling of two-phase flow in microchannels with nearly constant heat flux boundary conditions, J. Microelectromech. Syst. 11 (1) (2002) 12–17.
[6] G. Hetsroni, A. Mosyak, Z. Segal, Nonuniform temperature distribution in electronic devices cooled by flow in parallel microchannels, IEEE Trans. Components Packaging Technol. 24 (1) (2001) 17–23.
[7] G. Hetsroni, A. Mosyak, Z. Segal, G. Ziskind, A uniform temperature heat sink for cooling of electronic devices, Int. J. Heat Mass Transfer 45 (2002) 3275–3286.
[8] D. Wen, D.B.R. Kenning, Y. Yan, Flow boiling of water in a narrow vertical channel at low mass flux: observations of

local phenomena, Proceedings of the Twelfth International Heat Transfer Conference, France, 2002, pp. 773–778.
[9] D. Brutin, F. Topin, L. Tadrist, Experimental study on two-phase flow and heat transfer in capillaries, Proceedings of the Twelfth International Heat Transfer Conference, France, 2002, pp. 789–784.
[10] K. Suzuki, H. Saito, K. Matsumoto, K. Torikai, H. Maki, Subcooled flow boiling of water with microbubble emission in a horizontal channel, Proceedings of the Twelfth International Heat Transfer Conference, France, 2002, pp. 719–724.
[11] Y. Ding, S. Kakac, X.J. Chen, Dynamic instability of boiling two-phase flow in a single horizontal channel, Experimental Thermal and Fluid Science 11 (1995) 327–342.
[12] Q. Wang, X.J. Chen, S. Kakac, Y. Ding, Boiling onset oscillation: a new type of dynamic instability in a forced-convection upflow boiling system, Int. J. Heat Fluid Flow 17 (4) (1996) 418–423.
[13] H. Yuncu, O.T. Yildirim, S. Kakac, Two-phase flow instabilities in a horizontal single boiling channel, Appl. Sci. Res. 48 (1991) 83–104.
[14] P.R. Mawaha, R.J. Gross, Periodic oscillations in a horizontal single boiling channel with thermal wall capacity, Int. J. Heat Fluid Flow 22 (2001) 643–649.
[15] J.M. Kim, S.Y. Lee, Experimental observation of flow instability in a semi-closed two-phase natural circulation loop, Nucl. Eng. Des. 196 (2000) 359–367.